AFRL-RZ-WP-TP-2007-248

NON-REACTING AND COMBUSTING FLOW INVESTIGATION OF BLUFF BODIES IN CROSS FLOW (POSTPRINT)

Barry Kiel, Kyle Garwick, Amy Lynch, and James R. Gord, Ph.D.

Combustion Branch
Turbine Engine Division

AUGUST 2007

AIR FORCE RESEARCH LABORATORY
PROPULSION DIRECTORATE
WRIGHT-PATTERSON AIR FORCE BASE, OH 45433-7251
AIR FORCE MATERIEL COMMAND
UNITED STATES AIR FORCE

REPORT DOCUMENTATION PAGE

Form Approved
OMB No. 0704-0188

1. REPORT DATE *(DD-MM-YY)*	2. REPORT TYPE	3. DATES COVERED *(From - To)*
August 2007	Conference Paper Postprint	01 August 2005 – 01 August 2007

4. TITLE AND SUBTITLE
NON-REACTING AND COMBUSTING FLOW INVESTIGATION OF BLUFF BODIES IN CROSS FLOW (POSTPRINT)

5a. CONTRACT NUMBER
In-house

5b. GRANT NUMBER

5c. PROGRAM ELEMENT NUMBER
62203F

6. AUTHOR(S)
Barry Kiel, Kyle Garwick, Amy Lynch, and James R. Gord, Ph.D. (AFRL/RZTC)
Terrence Meyer, Ph.D. (Innovative Scientific Solutions, Inc.)

5d. PROJECT NUMBER
3066

5e. TASK NUMBER
05

5f. WORK UNIT NUMBER
306605YY

7. PERFORMING ORGANIZATION NAME(S) AND ADDRESS(ES)

Combustion Branch (AFRL/RZTC), Turbine Engine Division
Air Force Research Laboratory, Propulsion Directorate
Wright-Patterson Air Force Base, OH 45433-7251
Air Force Materiel Command, United States Air Force

Innovative Scientific Solutions, Inc.
Dayton, OH

8. PERFORMING ORGANIZATION REPORT NUMBER
AFRL-RZ-WP-TP-2007-248

9. SPONSORING/MONITORING AGENCY NAME(S) AND ADDRESS(ES)
Air Force Research Laboratory
Propulsion Directorate
Wright-Patterson Air Force Base, OH 45433-7251
Air Force Materiel Command
United States Air Force

10. SPONSORING/MONITORING AGENCY ACRONYM(S)
AFRL/RZTC

11. SPONSORING/MONITORING AGENCY REPORT NUMBER(S)
AFRL-RZ-WP-TP-2007-248

12. DISTRIBUTION/AVAILABILITY STATEMENT
Approved for public release; distribution unlimited.

13. SUPPLEMENTARY NOTES
Conference paper published in the Proceedings of the 42nd AIAA/ASME/SAE/ASEE Joint Propulsion Conference and Exhibit.

PAO Case Number: AFRL/WS 06-1677, 06 Jul 2006.

14. ABSTRACT
This paper is the first in a series of papers studying the behavior of bluff body stabilized flames. In this research a combination of Laser Doppler Velocimetry (LDV), and High Speed Imaging are used to investigate these flames. LDV data taken over several non-combusting operating conditions detail the recirculation zone behind the bluff body as well as the effect of inlet conditions on the Karman Street vortex shedding that occurs. High speed images of combustion and equivalence ratio taken at blow out agree with assertions made by Ozawa (1971) and Zukoski (1957) on the transitional nature of the flame from "laminar" to "turbulent" at a Reynolds number of around 15,000. Lean blow out also correlate very well when using the correlation parameter set down by Dezubay (1950). Finally, high speed images also support assertions by Mehta and Soteriou (2003) Erickson et al. (2006) that under certain conditions Karman Street vortex shedding is not suppressed by momentum and baroclinic effects and are present in the flame near lean blowout.

15. SUBJECT TERMS

16. SECURITY CLASSIFICATION OF:			17. LIMITATION OF ABSTRACT:	18. NUMBER OF PAGES	19a. NAME OF RESPONSIBLE PERSON (Monitor)
a. REPORT	b. ABSTRACT	c. THIS PAGE			Lt. Kyle Garwick
Unclassified	Unclassified	Unclassified	SAR	18	19b. TELEPHONE NUMBER *(Include Area Code)* N/A

Standard Form 298 (Rev. 8-98)
Prescribed by ANSI Std. Z39-18

42nd AIAA/ASME/SAE/ASEE Joint Propulsion Conference & Exhibit
9 - 12 July 2006, Sacramento, California

2006 AIAA/ASME/SAE/ASEE Joint Propulsion Conference
9-12 July, 2006, Sacramento, California

Non-Reacting and Combusting Flow Investigation of Bluff Bodies in Cross Flow

Barry Kiel, Kyle Garwick, Amy Lynch, and James R. Gord, Ph.D.
Air Force Research Laboratory
Wright Patterson Air Force Base

Terrence Meyer, Ph.D.
Innovative Scientific Solutions, Inc.
Dayton, OH

ABSTRACT

This paper is the first in a series of papers studying the behavior of bluff body stabilized flames. In this research a combination of Laser Doppler Velocimetry (LDV), and High Speed Imaging are used to investigate these flames. LDV data taken over several non-combusting operating conditions detail the recirculation zone behind the bluff body as well as the effect of inlet conditions on the Karman Street vortex shedding that occurs. High speed images of combustion and equivalence ratio taken at blow out agree with assertions made by Ozawa (1971) and Zukoski (1957) on the transitional nature of the flame from “laminar” to “turbulent” at a Reynolds number of around 15,000. Lean blow out also correlate very well when using the correlation parameter set down by Dezubay (1950). Finally, high speed images also support assertions by Mehta and Soteriou (2003) Erickson et al. (2006) that under certain conditions Karman Street vortex shedding is not suppressed by momentum and baroclinic effects and are present in the flame near lean blowout.

1 INTRODUCTION

Flame stabilization by a bluff body is commonly used in propulsion systems including gas turbine and scram jet engines. Models are used to estimate the effectiveness of these stabilization methods. These modes vary in sophistication from simple empirical expressions to the solution of detailed partial differential equations. The accuracy of these models depends on extent the models are validated. Equally as important, these models are also only as accurate as the physical phenomenology the models capture.

For the past fifty years bluff body stabilized flames have been studied in detail. In the 1950s DeZubay (1950) and King (1957), studied flames stabilized using bluff bodies. Both authors found that the fuel air ratio the flame blows out at correlates with the inlet pressure, temperature, and velocity, see Figure 1-1.

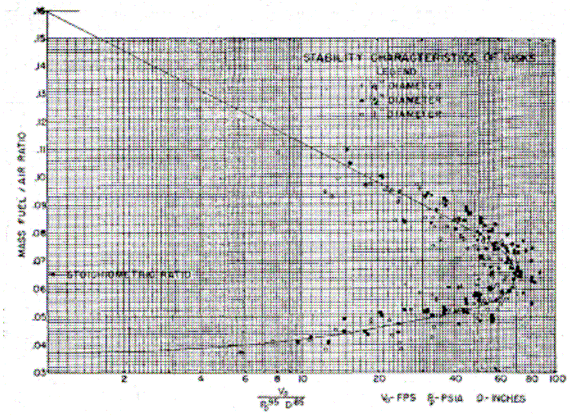

Figure 1-1 Dezubay’s Blowout Correlation (Dezubay 1950)

In this work the authors studied blowout at relatively high Reynolds numbers. Dezubay studied a round disk shaped flame holders over a range of Reynolds numbers from 90,000 to 680,000. King on the other hand studied a v-shaped bluff body over a range of Reynolds Numbers from 60,000 to 130,000.

Due to the increasing inlet temperatures Reynolds numbers for modern systems are much lower than those of the 1960s and 1970s. Reynolds numbers vary typically in the range of 15,000 to 300,000. In his work Zukoski (1954, 1955) studied blowout. He found that the blow out characteristics behave quite differently at lower Reynolds numbers. Zukoski concludes that the flame transitions around a Reynolds numbers of 10,000. Later Ozawa (1971) also compiled data from several bluff body experiments. Ozawa also discusses this blowout transition at Reynolds Number of 10,000. Both authors conclude the flame surface transitions from “laminar” to “turbulent” near this Reynolds number. Further, they both

concluded that this transition greatly effects the velocity at which the flame will blow off at, or the characteristic of the blow-out curve.

More recently Mehta and Soteriou (2003), and Erickson et al. (2006) have commented on vortex shedding as it relates to bluff body flame blow-out. I their work they have conducted detailed modeling of bluff body stabilized flames. In their 2003 work they concluded that the baroclinic effect of the temperature rise across the flame suppresses the Karman Street type vortex shedding typically seen behind these bluff bodies under non-combusting conditions. In this paper they modeled a bluff body flame at 20,000 Reynolds number. They concluded that the flame was dominated not by large Karman Street vortices but much smaller vortices. They also concluded that the baroclinic torque generated by the temperature rise across the flame was responsible for suppressing the Karma Street vortex production.

Later in 2006, (Ericson et al. (2006)) they conducted another model study where the temperature rise across the flame was varied. In this study they concluded that at lower temperature ratios across the flame, the flame near blowout was dominated not by small turbulent vortices but by large Karman Street type vortices. These same structures were also captured by Porumbel and Menon (2006), and Fureby (2006) in their combusting Large Eddy Simulation (LES) investigations.

The objective of this research effort is two fold. First the objective is to provide detailed experimental data on bluff body stabilized flames for model validation. Second the objective is to enhance the phenomenological understanding of these bluff body flame stabilization. In this paper a detailed study of the velocity patterns, vortex shedding and blowout v-gutter bluff bodies is studied over a large range of Reynolds numbers, from 5,000 to 60,000. Detailed LDV data are collected of cold flow in the wake the v-gutters. From the LDV, mean, RMS, and turbulent spectra are collected. Combusting experiments are also conducted over the same range of Reynolds numbers. High Speed images of the flame just prior to blow out are recorded as are the equivalence ratio at blowout.

2 PROCEDURES

2.1 LDV Procedures

A two-component LASER Doppler Velocimetry (LDV) system was employed for measuring instantaneous velocity at various conditions in the wake region of the flame holder, Figure 2-1. The LDV system is driven by an argon-ion LASER with 514.5 nm and 488 nm output beams. When focused on a small control volume, the 514.5 nm and 488 nm beams generate orthogonal interference fringes from scattering off 1 micron aluminum oxide particles used to seed the flow. For a more detailed discussion of principles of LDV please reference Goldstein (1983).

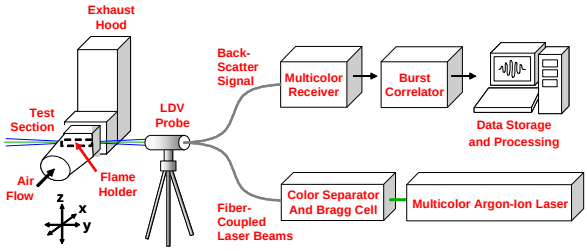

Figure 2-1. LASER Doppler Velocimetry Set-up.

2.2 Analysis of Randomly Time Sampled LDV Data

The quality of data from LDV depends on several factors, the most important of which is the seed density of the flow. In areas of recirculation seed density can vary so much as to produce periods of time where there are few velocity data. When the seed conditions are poor data can not be taken at a known interval of time, but must be collected at the time of arrival of the each particle. Figure 2-2 depicts a a sample histogram of the various time intervals present in LDV data.

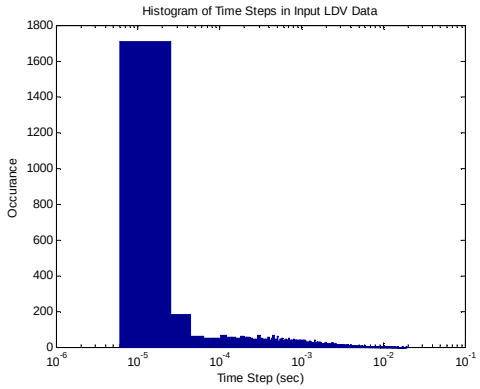

Figure 2-2. Histogram of Time Steps in LDV Data.

In this experimental campaign LDV is used to produce mean and RMS velocity data and the shedding frequency of the coherent vortex shed

behind the bluff body. For the mean and RMS velocities simple mathematical functions can be employed to obtain these parameters from the LDV data taken at each point. For the shedding frequency of the coherent vortex the data analysis is not as straight forward. Because the time interval produced by LDV is random, standard DFFT techniques can not be used to analyze LDV data. The spectral analysis of randomly spaced LDV data is traditionally conducted using the Lomb Algorithm for spectral analysis (Numerical Recipes in C, 1992).

In this experiment the entire spectrum of turbulence is not required to determine the shedding frequency of the coherent vortex. To obtain the shedding frequency, spectrum up to three times the shedding frequency is required to satisfy Nyquest. This results in maximum frequencies required on the order of 200-400 Hz. Because of this simpler techniques are used to analyze the data. A technique is used where the data are resample onto a uniformly spaced time interval through the use of cubic Hermite interpolation. The time step of the interpolation was chosen based the histogram of the time steps of the randomly spaced LDV data and the median of the time step data. An FFT of the interpolated velocity then performed in MATLAB. When compared to spectral data produced with the Lomb Algorithm, there was excellent agreement between the two, as will be discussed in a future paper.

3 EXPERIMENTAL SETUP

A 12MW experimental combustion facility located at the Propulsion Directorate of AFRL in Wright-Patterson Air Force Base, Dayton Ohio was used for the experiments, Figure 3-1. Flow conditioning is employed in the facility which provides a uniform velocity and temperature profile (± 3%), and 6-7% turbulence at the inlet of the test section. Tests were conducted on an "open and "closed" v-gutter bluff body mounted in the rig, see Figure 3-2. In these tests the flame holder traverses the length of the test section. In this configuration the flow is considered two-dimensional at the center of the test rig. Combustion tests were conducted with premixed propane and air.

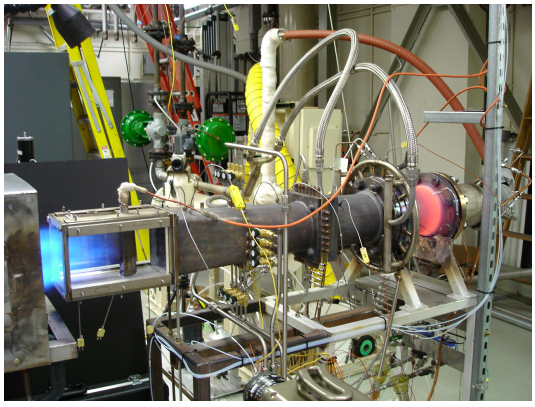

Figure 3-1 12 MW Experimental Test Facility

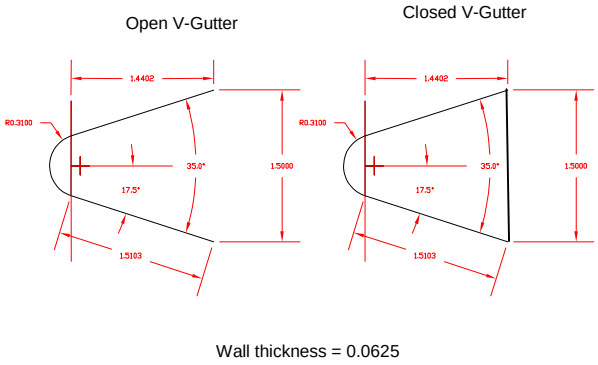

Figure 3-2. Open and Closed V-Gutter Flame Holders

4 DATA ANALYSIS

4.1 Mean and RMS Profiles

Detailed Velocity profiles were taken using LDV behind the non reacting wake of the v-gutters. Traverses were taken parallel and transverse to the centerline axes of the test section. Figure 4-1 depicts the location of these traverses. The orange traverses in Figure 4-1 are perpendicular to the centerline of the test section traversing across the wake of the bluff body. The green traverse in Figure 4-1 is parallel to the centerline of the test section.

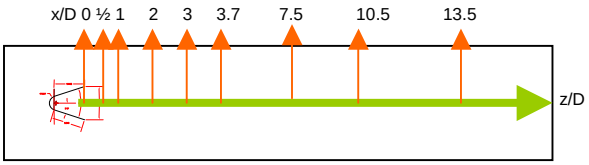

Figure 4-1 Locations of Velocity Traverses

Figures 4-2 and 4-3 are plots of mean and RMS axial velocity respectively along the "green" traverse in Figure 4-1. The gaps in both sets of data represent sections of the test

section where there was no optical access for the LDV LASER. Figure 4-2 depicts the mean velocity normalized by the inlet velocity. Figure 4-3 depicts the RMS normalized by the inlet velocity. The data presented are for 4 Reynolds numbers; 10,000, 25,000, 40,000, and 55,000. The mean axial velocity changes substantially from the near wake to the far wake region. From the trailing edge of the flame holder the mean velocity is increasingly negative, reaches a maximum then increases to zero. The location where the velocity is zero represents the mean location of the trailing edge of the recirculation zone behind the bluff body. Note as the Reynolds number increases the length of the recirculation zone decreases. The location of the maximum negative velocity also moves closer to the trailing edge of the bluff body as the Reynolds number increases. In the far wake region the velocity increases asymptotically to

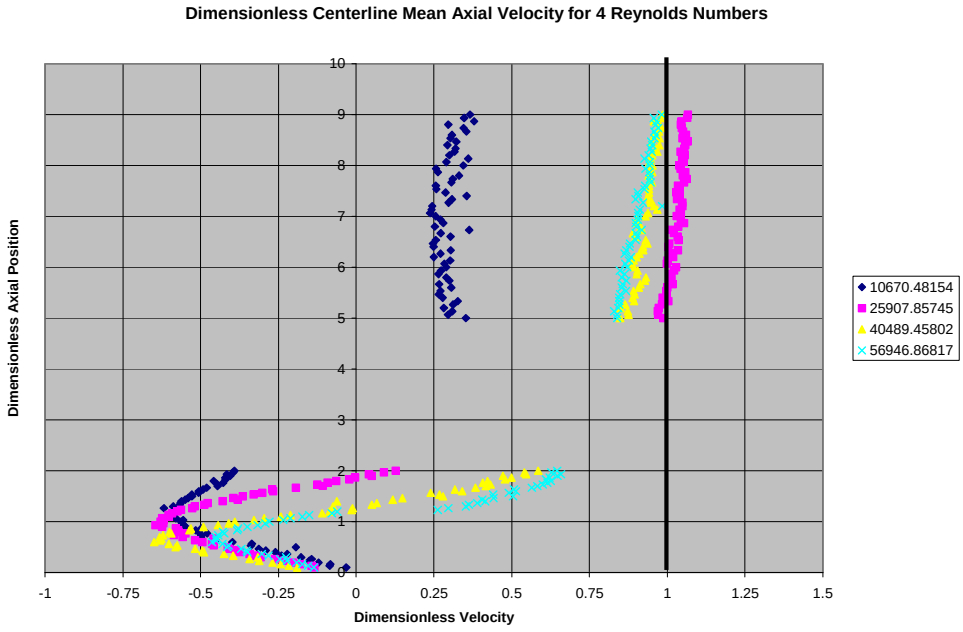

Figure 4-2 Travers of Axial Velocity Behind the Bluff Body

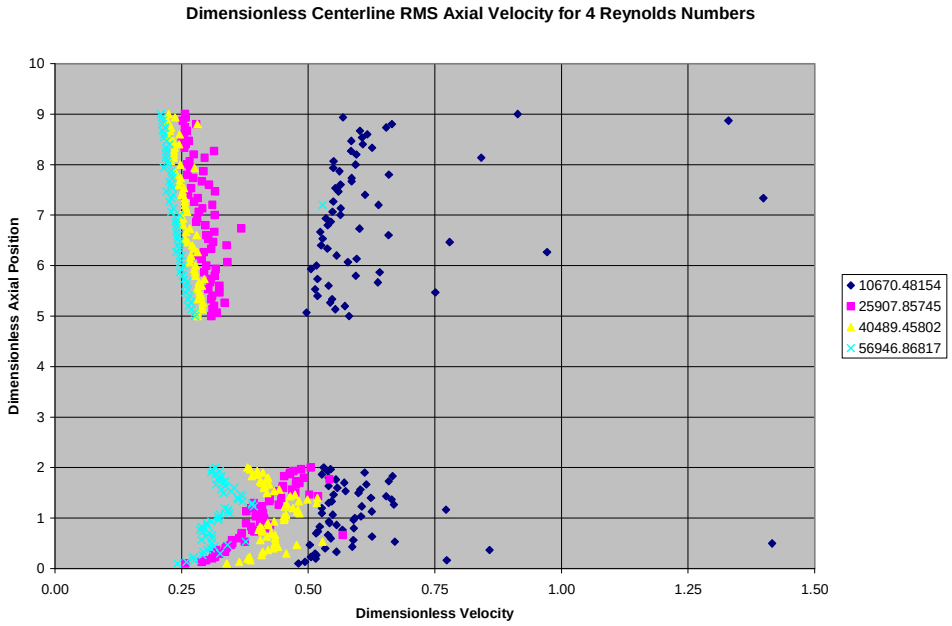

Figure 4-3 Traverse of RMS Velocity Behind the Bluff Body

the inlet velocity for all but the 10,000 Reynolds number case. In the case of Reynolds number 10,000 the low velocity wake persists the entire length of the test section behind the flame holder.

The RMS velocity also varies as the Reynolds number increases. For the lowest Reynolds number, 10,000, the wake is highly turbulent. For this Reynolds number the RMS velocity is routinely greater than 50% of the inlet velocity in the wake of the bluff body for the entire length of the test section. There is also a lot of scatter in the data due to the low data rate that occurred for many of these points. For the higher Reynolds numbers the RMS velocity is more similar.

For the higher Reynolds number cases the RMS velocity has two relative maximums in the recirculation zone. Both maxima occur at the location where the derivative of the mean velocity is zero. The second maximum is higher than the first and represents the highest RMS value in the wake of the bluff body. In the far wake the RMS are still highly turbulent but turbulence is decaying. RMS values continue to decrease, below 25% 9 flame holder width's down stream of the bluff body.

Velocity profiles were also taken across the wake down stream of the bluff body, see the orange lines in Figure 4-1. Figures 4-4 to 4-6 depict the mean and EMS velocity profiles for 0.5L, 1.0L, and 2.0L down stream of the bluff body for a Reynolds number of 40,500. On the left of each figure are plots of mean and RMS velocity along the centerline axis while on the right are the mean and RMS of the transverse 0.

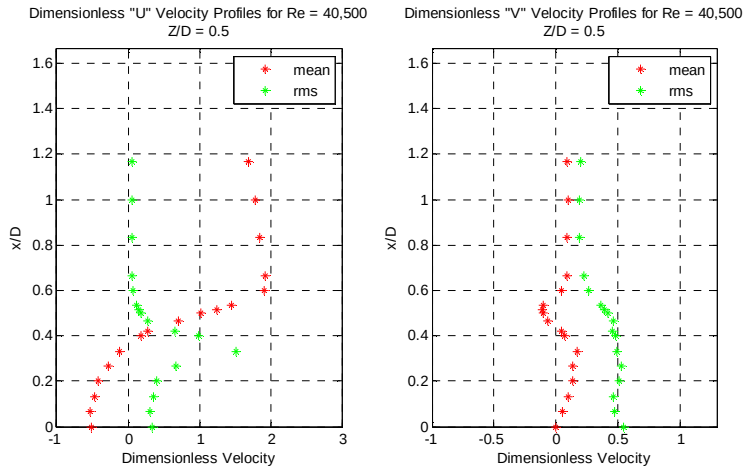

Figure 4-4 Velocity Profiles Z/D = 0.5 Down Stream of the Bluff Body for Reynolds Number = 40,500

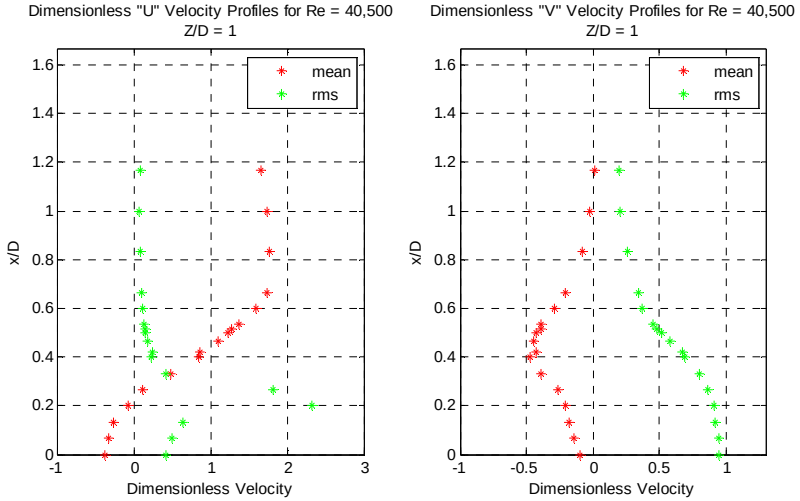

Figure 4-5 Velocity Profiles fro Z/D = 1 Down Stream of the Bluff Body for Reynolds Number = 40,500

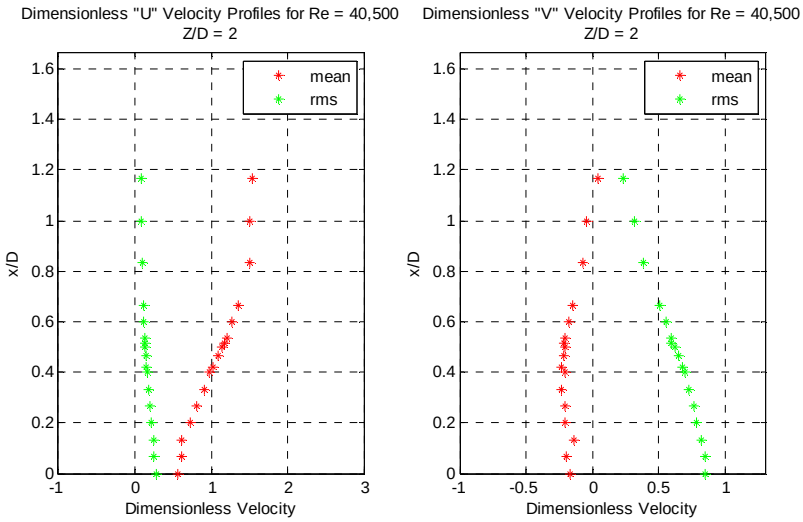

Figure 4-6 Velocity Profiles fro Z/D = 2 Down Stream of the Bluff Body for Reynolds Number = 40,500

velocity. Data were also taken for Reynolds numbers of 10,000, 12,000, and 55,00

There are several points of interest in these figures. Figure 4-4, depicts the mean axial velocity L/2 down stream of the trailing edge of the bluff body. The edge of the bluff body is located at X/D = 0.5. At this point the velocity is approximately the same as the inlet velocity. Further away from the flame holder the velocity reaches a maximum of almost 2 times the inlet velocity. In this experiment the blockage ratio of the flame holder is approximately 1.43. Thus the "lip velocity" is higher than the velocity expected assuming an acceleration due to the blockage.

Also of note is the RMS velocity. In all three figures the RMS of the axial velocity reaches a maximum inside the wake of the flame holder. Close to the bluff body this maximum can be twice the inlet velocity, or 200%. The transverse RMS velocity also reaches a maximum in the wake region. Unlike the axial RMS the transverse RMS persists well outside the wake. A detailed analysis of the LDV supplemented with PIV data is the subject of a future paper.

4.2 LARGE COHERENT STRUCTURES

Another important aspect of the fluid dynamics of a bluff body in cross flow is the large Karman Street vortex seen shed in the wake of the bluff body. LDV was conducted over a wide range of Reynolds number for both the open and closed v-gutter bluff bodies. The shedding frequency for a given Reynolds number was found by taking the DFFT of each set of interpolated data, as outlined in section 2. The frequency was then non-dimensionalized to Strouhal number using the effective or blockage velocity, not the inlet velocity, and the width of the v-gutter. Figure 4-7 is a plot of this data. Also plotted in Figure 4-7 are the data for a circular cylinder in cross flow for reference, Blevins (1985).

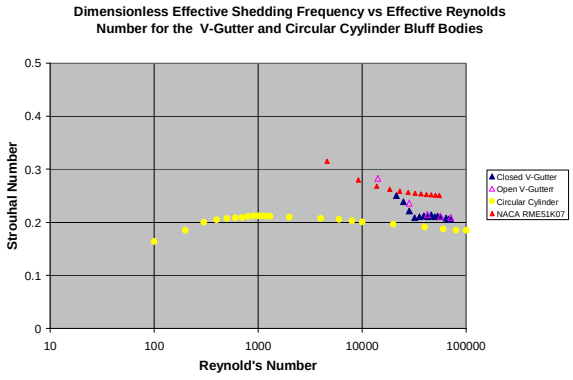

Figure 4-7. Dimensionless Shedding Frequency Several Reynolds Numbers.

4.3 LEAN BLOWOUT

Detailed lean blowout measurements were also taken for the combusting v-gutters. Figure 4-8 depict the equivalence ratio recorded at lean blow out (LBO) versus Reynolds Number for the

closed v-gutter flame holder at 4 different temperatures. In all cases the data plotted represent the average of at least 6 blow out points for the given Reynolds number. Due to facility limitations the highest Reynolds number for the 70F, 300F, and 460F inlet temperatures were 55,000, 34,000, and 29,000 respectively.

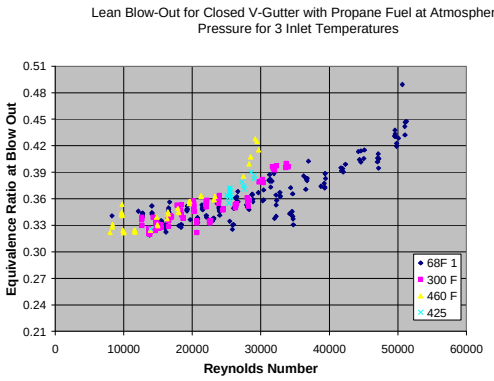

Figure 4-8 Lean Blow Out Equivalence Ratio vs. Reynolds Number for Several Inlet Temperatures

When studying Figure 4-8 two interesting results can be discerned. At lower Reynolds numbers, below 15,000 the lean blowout seems insensitive to Reynolds number. Above 20,000 Reynolds number, the LBO increases with increasing Reynolds number. Figure 4-9 depicts the LBO data plotted against the DeZubay correlation parameter instead of Reynolds number. When plotted this way the data correlate very well, similar to the shape of DeZubay's original data.

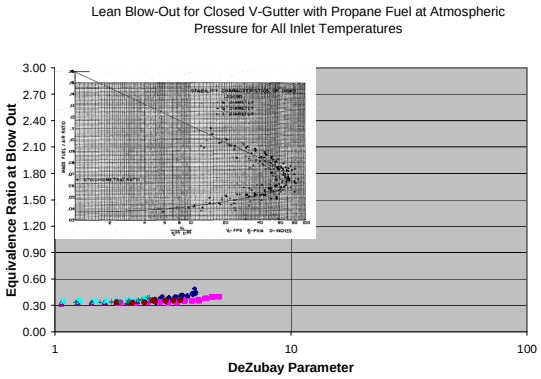

Figure 4-9 Lean Blow Out Equivalence Ratio vs. DeZubay Correlation Parameter

Another very interesting trend can be seen in Figure 4-8. As the inlet temperature increases for a given Reynolds number the equivalence ratio at LBO increases. Intuitively one would expect this value to decrease with temperature, not increase. Ballal and Lefebvre (1979) studied the relationship between temperature and weak extinction for constant inlet velocity. They found the extinction limit decreases with inlet temperature. Figure 4-10 depicts the equivalence ratio at LBO for a constant inlet velocity of 25 m/s for several inlet temperatures. When plotted this way the equivalence ratio at LBO does show the expected decreasing trend.

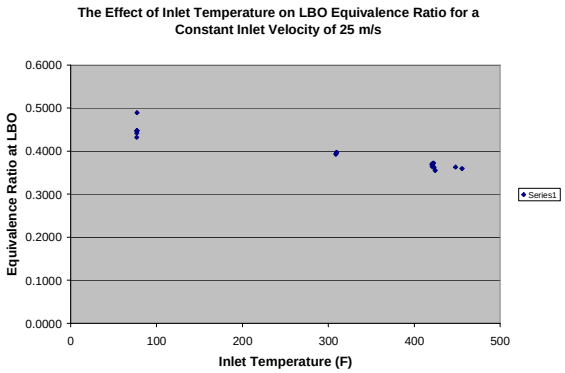

Figure 4-10 Lean Blow Out Equivalence Ratio vs. Inlet Temperature for Several Inlet Temperatures

4.4 HIGH SPEED IMAGES

Many high speed images were also taken of the flame behind the closed v-gutter flame holder with a Phantom 7.2 camera. Flame intensity images were captured at 5KHz. Figure 4-11 is a typical high speed image the flame behind a v-gutter bluff body with combustion. For this image the inlet temperature was, 70F, the Reynolds number is approximately 30,000 and the equivalence ratio 0.64. Note the flame is dominated by smaller vortices that seem to be generated by the boundary layer. This flame is absent of the large Karman Street vortices

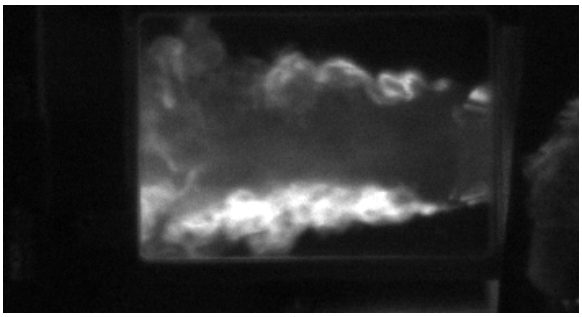

Figure 4-11 High Speed Image of Combusting V-Gutter at Higher Equivalence Ratio

typical of a non-combusting flow. This figure is representative of Reynolds numbers greater than 15,000 for equivalence ratios well above the lean limit. Figure 4-12 is a high speed image of the same conditions as Figure 4-10 near LBO, an equivalence ratio of 0.35. The flame structure of both images is very similar. In both images vortices are clearly seen in the shear layer and there is very little vortex motion in the wake region.

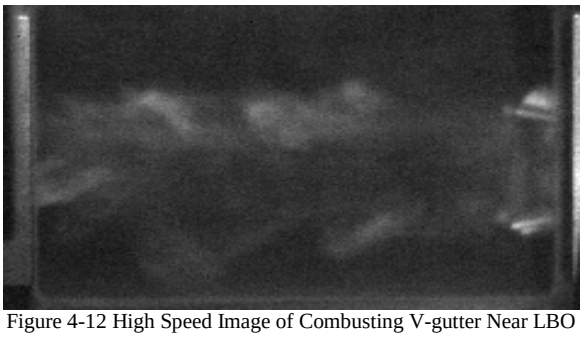

Figure 4-12 High Speed Image of Combusting V-gutter Near LBO

High speed images were also taken at elevated inlet temperatures. Figures 4-13 and 4-15 are images the flame near LBO for Reynolds number 26,000 and 32,000 respectively at an inlet temperature of 70F. In both of these images the largest vortices are those in the shear layer generated by the boundary layer of the flow. Figures 4-14 and 4-16 are images near LBO for Reynolds number is 25,000 and 35,000. In these images the inlet temperature was elevated to 460F with electric heaters. Note in these images one can easily see large vortices in the wake of the flame holder reminiscent of Karman Street vortices shed behind the bluff body without combustion.

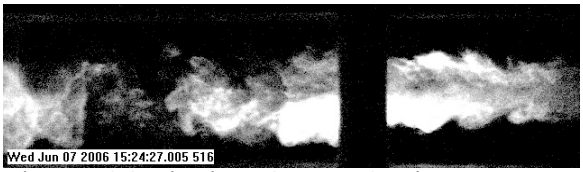

Figure 4-13 Combusting V-Gutter at 70F Inlet Temperature, Re = 26,000, Near LBO

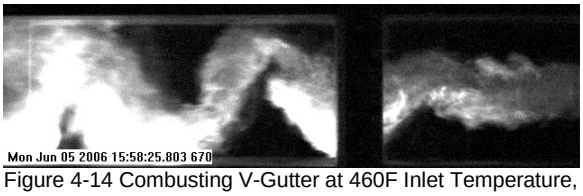

Figure 4-14 Combusting V-Gutter at 460F Inlet Temperature, Re = 25,000, Near LBO

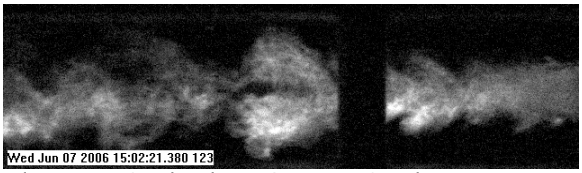

Figure 4-15 Combusting V-Gutter at 70F Inlet Temperature, Re = 32,000, Near LBO

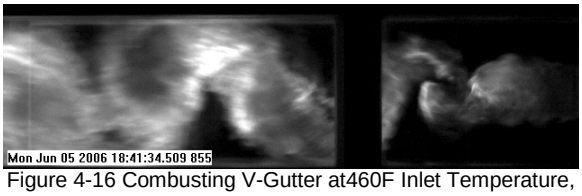

Figure 4-16 Combusting V-Gutter at460F Inlet Temperature, Re = 35,000, Near LBO

This contrast is representative of the many high speed images taken above a Reynolds number of 15,000 for 70F and 460F inlet temperatures.

At lower Reynolds numbers the vortex shedding phenomena at LBO is different from those above Reynolds number of 15,000. Figures 4-17 and 4-18 are high speed images taken near the LBO limit. They depict Reynolds

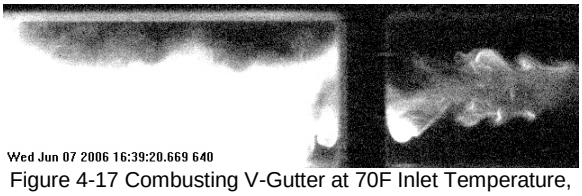

Figure 4-17 Combusting V-Gutter at 70F Inlet Temperature, Re = 8,300, Near LBO

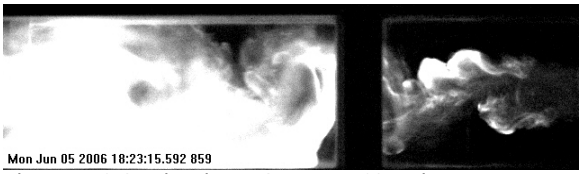

Figure 4-18 Combusting V-Gutter at 460F Inlet Temperature, Re = 9,700, Near LBO

numbers of 8,300 and 9,600 and inlet temperatures of 70F and 460F respectively. Both of these images seem to be dominated by a combination of large and small vortices. It is difficult to discern a dominant vortex shedding mode.

5 CONCLUSIONS AND RECOMMENDATIONS

In this paper, several sets of data were presented for the closed flame holder. Experiments are ongoing to collect similar data for the open v-gutter configuration, a circular

cylinder and other bluff body configurations. In addition new instrumentation is also planned to collect point temperature and species measurements.

Currently analysis of this data and data from the open v-gutter flame holder are ongoing. From the data currently analyzed and presented conclusions can be drawn. Enough data are believed to exist to provide "necessary" conclusions. More data and analysis is required to provide conclusions that are supported by data that is both "necessary" and "sufficient". Given this, some interesting conclusions can be drawn from the data and analysis to date.

5.1 Turbulent Transition

Fluid dynamic transition of the v-gutter flame holders varies substantially from that of the circular cylinder. The slope of the curve at lower Reynolds numbers is discontinuous, unlike the circular cylinder. For a circular cylinder, the vortex shedding may be very different than that of a v-gutter. When comparing Panton's (1984) discussion of vortex shedding behind a circular cylinder with the data from Blevins (1985), the peak in Strouhal number for a circular cylinder occurs at a Reynolds number where there is still a very organized Karman Street vortex shed behind the cylinder. According to Panton (1984), as the Reynolds number increases the boundary layer of the cylinder separates. Also, as Reynolds number increases the point of separation moves forward. At the same time the separation moves forward on the cylinder the Strouhal number decreases. Panton concludes the flow behind the cylinder is not "turbulent" until the Reynolds number approaches 30,000.

The v-gutter data does not depict the same smooth decrease in Strouhal number as Reynolds number increases. Between Reynolds numbers of 20,000 and 25,000 there is a cusp in the shape of the curve denoting an abrupt change in the vortex shedding. This may be the transition from "laminar" to "turbulent" shedding in the wake for the v-gutter. These conclusions can be supported by better visualization around the range of Reynolds numbers where the cusp in the data occurs. This can be accomplished with highly spatially resolved Large Eddy Simulation (LES) or through the use of Particle Image Velocimetry (PIV) analysis of a v-gutter and a circular cylinder. Since this transition occurs at the lower range of Reynolds numbers for current engines this is an area of further research.

As outlined in the Introduction, Zukoski (1954, 1955) and Ozawa (1971) concludes that the flame behind a bluff body transitions around a Reynolds numbers of 10,000. In the equivalence ratio data presented, the equivalence ratio at LBO below Reynolds number of 15,000 seem to be insensitive to Reynolds number supporting these conclusions. The high speed images in this Reynolds range also contain a mix of vortices being shed by the shear layer of the flame holder and larger wake vortices. When compared to high speed images at higher Reynolds numbers the images also seem to support the conclusions that the flame transitions in this Reynolds range.

Reynolds numbers below 10,000 are rarely achieved in modern engines, thus this conclusion may be academic. Regardless the ability to collect data at these conditions is relatively easy. Further data will be collected on different flame holder geometries and at different conditions in an attempt to further support this conclusion. Other instrumentation can be used to shed further light here. In addition to high speed imaging, Particle Image Velocimetry (PIV) of the combusting flow and highly temporally resolved temperature measurements may be applied at Reynolds numbers below "transition". The added data provided may shed more light as to the nature of the vortex shedding behind the bluff body.

5.2 Lean Blowout

From the lean blow out data two conclusions are drawn. The first is that the blow out data correlate well when DeZubay's correlation is used. The maximum correlation parameter value of 30 was achieved in the current testing. Research will continue at higher inlet temperatures and velocities to continue to populate this curve at correlation values greater than 30.

When plotted against Reynolds number the data seem counter intuitive. At higher temperatures, for the same Reynolds number the equivalence ratio at LBO are higher, not lower. When plotted against temperature, with constant inlet velocity, the equivalence ratio decreases with inlet temperature. This result would indicate that using the Reynolds number to correlate LBO does not properly account for

the competing effects of decreased density and increased viscosity as the temperature is increased.

5.3 Vortex Shedding in the High Speed Images

In their earlier paper Mehta and Soretiou (2003) concluded that the vortex shedding behind a bluff body changed substantially when combustion was present. They concluded that the baroclinic torque associated with the temperature rise across the flame dominated the flow. As a result their model showed a flame where flow behind the bluff body was dominated by vortices much smaller than the Karman Street vortices. At stoichiometry well above the LBO limit the high speed images seem to support this conclusion.

Later Mehta and Soteriou (Erickson et al. 2006) concluded from their modeling that certain conditions could exist where the flame could be dominated by the Karman Street vortices. They concluded that if the temperature ratio across the flame were reduced that these vortices eventually dominate the flow. This phenomenology is also supported by LES computations by Porumbel and Menon (2006), and Fureby (2006). High speed images qualitatively support these conclusion as well.

In the bluff body flow three forces seem to dominate depending on the operating conditions; momentum, viscous and baroclinic. For the high equivalence ratio combusting flow, above Reynolds number of 15,000, momentum and baroclinic forces seem to dominate. These forces suppress Karman Street vortex shedding and promote smaller vortices that stabilize the flame in the shear layer of the wake. As the inlet temperature is increased density falls and viscosity increases. Thus increased temperature decreases momentum and increases viscous effects. Further as inlet temperature increases the temperature ratio across the flame decreases for the same stoichiometry. The resultant effect is a reduction in the baroclinic effect of the flame. Combined the high speed images and modeling seem to support a situation where viscous forces and Karman Street vortex shedding dominate the combusting near LBO at Reynolds numbers as high as 35,000. Further testing using PIV in combusting flow as well as temporally resolved point temperature measurements are required to provide more quantitative results to support these conclusions.

6 REFERENCES

Adrian, R., 1983, “Laser Velocimetry,” in Fluid Mechanics Measurements, ed. R. J. Goldstein, Hemisphere Publishing Corporation, New York, pp. 155-244.

Ballal, D., and Lefebvre, A., 1979, “Weak Extinction Limits of Turbulent Heterogeneous Fuel/Air Mixtures”, Journal of Engineering and Power, 101, 3, p 343-348.

Blevins, 1985, “The Effect of Sound on Vortex Shedding from Cylinders”, *J. Fluid Mech*., Vol. 161, pp. 217-237.

DeZubay, E. A., 1950, “Characteristics of Disk-Controlled Flame,” *Aero Digest*, pp. 54-57.

Erickson, R., Soteriou, M., and Prashant, M., 2006, “The Influence of Temperature Ratio on the Dynamics of Bluff Body Stabilizee Flames”, AIAA 2006-753.

Fureby, C., 2006, “A Comparison of Flamelet LES Models for Premixed Turbulent Combustion”, AIAA 2006-155.

King, C. R., 1957, “A Semi Empirical Correlation of Afterburner Combustion Efficiency and Lean-Blowout Fuel-Air-Ratio with Several Afterburner Inlet Variables and Afterburner Lengths,” NACAE57RMF26.

Mehta, P.G., and Soteriou, M.C., 2003, “Combustion Heat Release Effects on the Dynamics of Bluff Body Stabilized Premixed Reacting Flows”, *AIAA 2003-0835*.

Numerical Recipes in C: The Art of Scientific Computing, 1992, Cambridge University Press, pp. 575-584 .

Ozowa, R. I., 1971, “Survey of Basic Data on Flame Stabilization and Propagation for High Speed Combustion Systems”, AFAPL-TR-70-81

Porumbel, I., and Menon, S. 2006, “Large Eddy Simulation of a Body Stabilized Premixed Bluff Flame:, AiAA 2006-0152

Roshko, A., 1954, “On the Drag and Shedding Frequency Two Dimensional Bluff Bodies”, NACA TN 3169

Younger G., Gabriel, D., and Mickelsen, W., 1951, Experimental Study of Isothermal Wake-Flow Characteristics of Various Flame Holder Shapes”, NACA RM E51K07.

Zukoski, E., 1954, “Experiments Concerning the Mechanism of Flame Blowoff From Bluff Bodies,” Thesis, California Institute of Technology

Zukoski, E., and Marble, F., 1955, “The Role of Wake Transition in the Process of Flame Staboilization on Bluff Bodies”, AGARD Combustion Research and Reviews, 167-180.